metals

MDPI

Article

# Free Volume Contributing to the Different Yield Behaviors between Tension and Compression Deformations in Metallic Glasses

**Pengwei Wang, Haiyang Li and Liang Yang ***

College of Materials Science and Technology, Nanjing University of Aeronautics and Astronautics, 210016 Nanjing, China; wangpengwei1288@outlook.com (P.W.); h_y_lee@nuaa.edu.cn (H.L.)

* Correspondence: yangliang@nuaa.edu.cn; Tel./Fax: +85-025-5211-2903

Received: 13 September 2017; Accepted: 16 October 2017; Published: 20 October 2017

**Abstract:** The different deformation behaviors in the yield stage, in particular, of metallic glasses under uniaxial tension and compression are investigated from an atomic structural perspective, by applying both experimental and simulation methods. A new computational approach for quantitatively calculating free volumes (FVs) in structural models is developed, based on which the manner in which FVs contribute to deformation is studied. It is found that FVs have different expansion behaviors in terms of their saturation sizes and corresponding strain values, which are essential structural causes of different yield behaviors in these two deformations in metallic glasses.

**Keywords:** metallic glasses; yield behavior; tension and compression; molecular dynamics; free volume

## 1. Introduction

Metallic glasses (MGs) have a number of attractive properties, such as high strength and hardness, wide elastic range, low internal friction, excellent corrosion and wear resistances, and so on [1,2]. However, the lack of tensile ductility at room temperature and the inability to offset catastrophic failure makes this class of alloys quasi-brittle materials [3,4]. It has been proposed in both experimental and theoretical investigations that tension and compression modes possess different yield behaviors [5–7]. Although studying the plasticity in tension or compression is still a long-standing issue, it has been suggested that the yield difference could be related to the difference in plasticity between tension and compression [8,9]. Therefore, it is necessary to the mechanisms of deformation—in the yield stage, in particular—for both tension and compression modes.

To research the microscopic deformation mechanism of MGs, various specific structural concepts have been proposed, including shear transformation zones (STZs), flow units, free volumes (FVs), and flexible volumes [10–14]. It is known that, beginning with the yield stage, STZs begin to form shear bands, which contribute significantly to the plasticity in MGs [9,15]. STZs are the fundamental units of plasticity in amorphous metals, and are small clusters of randomly close-packed atoms that spontaneously and cooperatively reorganize under the action of an applied shear stress. The continued propagation of shear strain occurs by a process of self-assembly; the operation of one STZ creates a localized distortion of the surrounding material, and triggers the autocatalytic formation of large planar bands of STZs, commonly called shear bands [16]. However, the atomic-scale processes underlying shear localization are difficult to study experimentally, due to the extremely short time and the very small length scales involved [15]. Since it has been suggested that FVs significantly affect the formation of STZs, it is reasonable to study the deformation mechanism from a FV perspective. Thus far, it has been difficult to quantitatively calculate FVs [17–19], because FV is an ambiguous and elusive concept. In our previous work, a method for quantitatively calculating atomic packing efficiency was developed [20], making it possible to quantitatively detect FVs, because atomic packing has a close relation to FVs [21].

In this work, a $Zr_2Cu$ composition is selected as the research prototype, because ZrCu is a well-known binary alloy system with a large glass-forming composition range, and usually has excellent mechanical properties. The yield strength difference between the tension and the compression deformations is studied, by using a molecular dynamics (MD) simulation and several synchrotron radiation experiments. By developing a new approach for calculating FVs quantitatively, it is found that FVs significantly contribute to the deformation in the yield stage.

## 2. Experimental and Simulation Section

An alloy ingot with composition $Zr_2Cu$ was fabricated by arc-melting Zr and Cu with purities of 99.9 wt % in a Ti-gettered high-purity argon atmosphere. The ingot was melted at least 5 times to ensure compositional homogeneity. The corresponding amorphous ribbons were prepared by melt-spinning, producing a cross section of $0.04 \times 2$ mm$^2$. Subsequently, a synchrotron radiation-based high-energy X-ray diffraction measurement was performed at beam line BW5, in HASYLAB, Hamburg, Germany. Furthermore, extended X-ray absorption fine structure (EXAFS) experiments for both Zr and Cu K-edge were carried out using a transmission mode at beam line BL14W1, at the Shanghai Synchrotron Radiation Facility, Shanghai, China, and U7C, at the National Synchrotron Radiation Laboratory (NSRL), Hefei, China.

It is known that MD simulation is a powerful tool for studying the structures and various properties of MGs, while usually lacking fitting of experimental data [8,22–27]. Meanwhile, reverse-Monte Carlo (RMC) simulation of the synchrotron radiation experimental data is another useful method for probing structural information in MGs, while the lack of chemical potential sometimes makes such calculation uncertain [20]. Therefore, to obtain a reliable structural model, a RMC method was adopted for simulating the synchrotron-radiation diffraction and EXAFS data, resulting in an initial structural model. Subsequently, a MD simulation was performed to modify this model. In detail, the LAMMPS software (2016 version, Sandia National Laboratories, Livermore, CA, USA) was used for this simulation, in which a realistic ZrCu embedded-atom method potential [28] was adopted. The initial model was relaxed in the NPT (constant number of particles, pressure, and temperature) ensemble [29] in this MD simulation under periodic boundary conditions, so that a modified as-prepared structural model was obtained. This scheme is similar to that applied for studying MGs in previous work [30].

Furthermore, this as-prepared structural model was deformed by another MD simulation, by applying a tensile or a compressive uniaxial strain at a rate of $1 \times 10^8$ s$^{-1}$ along the $x$-direction. The temperature was maintained at a constant value of 300 K. Periodic boundary conditions were imposed in both $y$- and $z$-directions. In this simulation, the ZrCu embedded atom method potential was applied.

## 3. Results and Discussion

The structural signals of the MD simulation for obtaining a modified structural model of $Zr_2Cu$ MG, coupled with those obtained from the synchrotron radiation experiments, are plotted in Figure 1. These structural signals include the structural factor ($S$(Q)), the total pair distribution function ($G$(r)), the Cu and Zr K-edge EXAFS signals. Both of the simulated $S$(Q) and EXAFS curves fit well with their experimental ones, indicating that such modified simulation can provide us with a more realistic structural model. According to this structural model, atomic- and cluster-level structural information can be deduced. All of the atoms are "frozen" in the simulated structural model, so that the positions and the sizes of atoms can be determined, making it possible to probe FVs.

The simulated uniaxial stress-strain curves of the $Zr_2Cu$ model under tension and compression are plotted in Figure 2. These simulated curves are in good agreement with those obtained in previous theoretical work, in terms of the elastic, yield, and plastic stages [31]. In both modes, there is a linear relation between stress and strain when the strain is <4%, implying an elastic deformation stage. With the increase of the strain, the rise in the stress values becomes slow, indicating an inelastic deformation. The stress reaches a maximum at a strain of about 8% in both tension and compression, denoting yield strength. When strain continues to increase, the strength drops, and reaches a

quasi-steady flow stress [7]. In the tension mode, the yield strength is ~2.5 GPa and the flow stress is ~1.8 GPa, whereas the counterparts in the compressive deformation are ~2.9 Gpa and ~2.1 Gpa. The lower yield strength under tension was also observed in both experimental [5,6] and simulation studies [16]. According to previous work [32], the difference between the yield strength and the quasi-steady flow stress is related to the degree of softening during deformation, and its magnitude reflects the propensity for strain localization in the flow region.

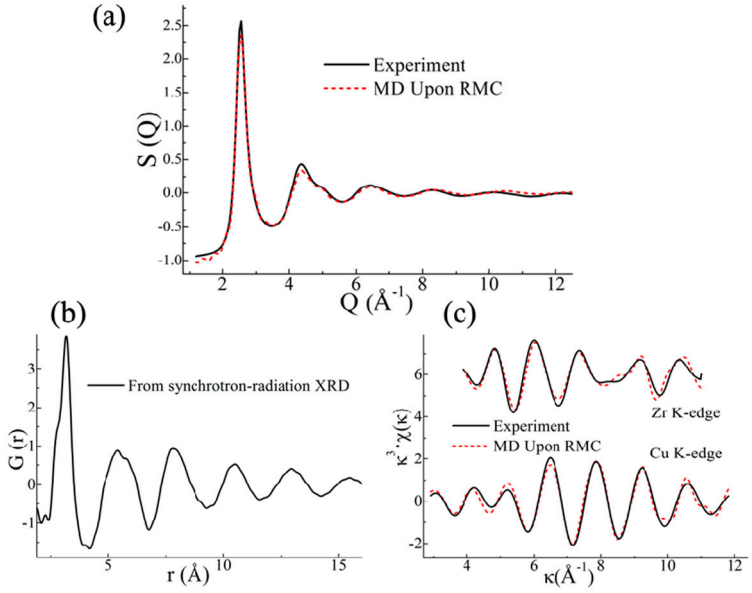


**Figure 1.** (Color online) Structural signals, including: (**a**) Structure factor, *S*(Q); (**b**) total pair distribution function, *G*(r); (**c**) Zr and Cu K-edge EXAFS (extended X-ray absorption fine structure) spectra. The solid and the dashed lines denote experimental and theoretical data, respectively. κ and χ(κ) represent the photoelectron wave vector and the κ-space EXAFS signal, respectively. This simulation was performed by MD (molecular dynamics) simulation to modify the RMC (reverse-Monte Carlo) initial model.

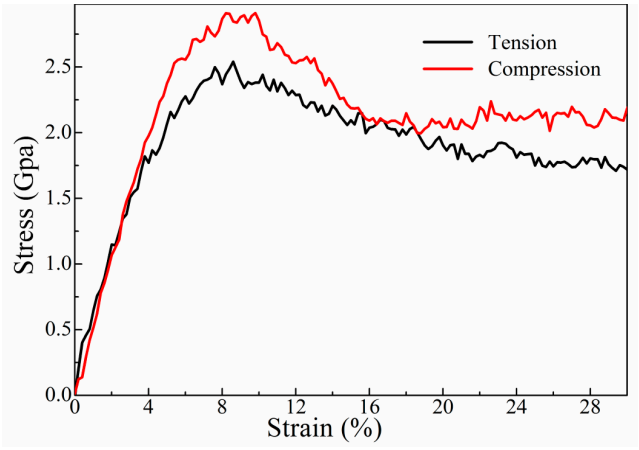


**Figure 2.** (Color online) The MD simulated uniaxial stress-strain curves of the $Zr_2Cu$ structural model under tension (Black solid line) and compression (Red solid line).

It is known that the deformations under the applied stresses are accompanied by some short-range structural changes in amorphous alloys [20,21,31–33]. To study short-range structural features at different deformation stages, the distribution evolution of various Voronoi clusters (VCs), which indicate the short-range order in MGs, was investigated using the Voronoi tessellation method [34].

Figure 3 shows the distribution of major VCs. It is observed that the change of the fractions of various VCs under tension is very similar to those of the compressed sample, which is in agreement with that observed in previous work [7]. Therefore, it is difficult to study the yield difference between tension and compression from a VC perspective. It is known that <0, 0, 12, 0> VC is the so-called full icosahedron, possessing full five-fold symmetries, and regarded as an indicator of high shear resistance, high packing density, and low potential energy [7,35]. In addition, it has been proposed that, during the deformation, both <0, 0, 12, 0> and some distorted icosahedral VCs, such as <0, 1, 10, 2>, which are densely packed units, will collapse to form loosely packed ones [7]. This leads to the formation of more excess FVs, which are finer structures in MGs. In this sense, it is necessary to examine why the yield strength in compression is higher than that of the tension, by quantitatively probing the FVs.

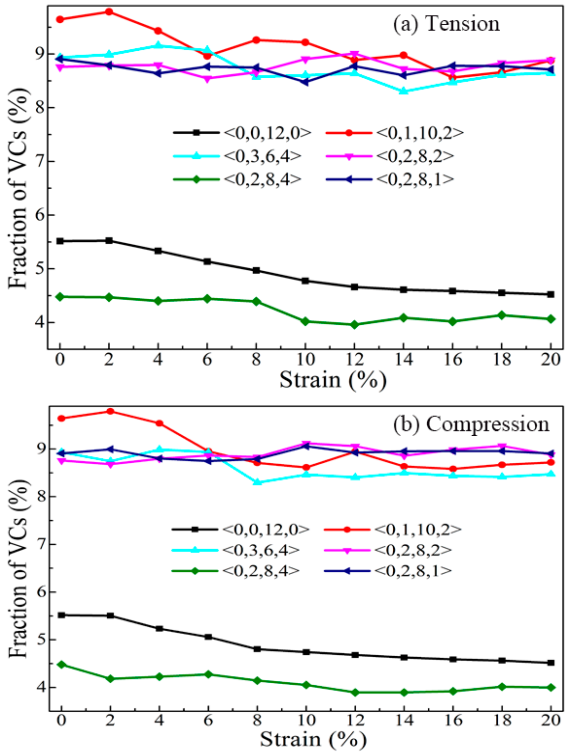


**Figure 3.** (Color online) Distribution of major Voronoi clusters during (**a**) tension and (**b**) compression.

In the present work, a new computational approach that can quantitatively detect FVs in MGs is designed. In the structural model, a hollow sphere with a changeable radius is adopted, which keeps on moving, in this model, until it touches any of the position-determined atoms, so that all of the void spaces between neighboring atoms can be detected. The center of each possible void is strictly defined. Any two neighboring void spaces whose center distances are too small or too large are merged or separated, so that the overlapping of small voids and the ignoring of large voids can be excluded. We emphasize that a void space itself cannot denote a FV directly [36]. These detected spaces are made up of both intrinsic voids and FVs. In other words, they represent the total void spaces not occupied by atoms [21].

It is known that there is a competitive crystalline phase in the composition of $Zr_2Cu$ [37], and it has been revealed that the devitrification phase of $Zr_2Cu$ MG is such a $Zr_2Cu$ tetragonal phase [38]. We assume that the intrinsic voids in the glassy state [21] will be similar to those in this crystal phase. All of the intrinsic voids in this $Zr_2Cu$ tetragonal phase are calculated, and are listed in Table 1. It is shown that, in the crystal model, there is no intrinsic void whose radius is larger than 0.4 Å, implying that intrinsic voids in the corresponding $Zr_2Cu$ MG should have radii shorter than 0.4 Å. In other words, any void space with a radius larger than 0.4 Å should be a FV, rather than an intrinsic void. In this way, relatively large FVs can be picked out. We emphasize that it is not correct to say that there

are no FVs with a size smaller than 0.4 Å. The number of void spaces with a size smaller than 0.4 Å in both the $Zr_2Cu$ crystal and amorphous models is calculated, and it is found that there is no obvious difference, suggesting that relatively small FVs can be ignored, in this case.

**Table 1.** Intrinsic voids calculated in a $Zr_2Cu$ tetragonal phase.

| Sample | Percentage (%) | | | |
|---|---|---|---|---|
| Size (Å) | ≤0.2 | 0.2–0.3 | 0.3–0.4 | ≥0.4 |
| $Zr_2Cu$ | 0 | 66.7 | 33.3 | 0 |

The average sizes of FVs (large voids whose radii are larger than 0.4 Å) corresponding to different strains of the structural model are calculated and plotted in Figure 4. Figure 4a shows the evolution of the average size of FVs in tension and compression. It is observed that the average size increases monotonously with the increase in strain in both tension and compression modes. It is worth noting that, in the tension mode, the average size increases from 0.604 Å to 0.637 Å, while the corresponding increase in compressive deformation is from 0.604 Å to 0.621 Å, implying that there is a rapid increase in FV size during tension. To further illustrate this, the changes in FVs corresponding to different strains in tension and compression are shown in Figure 4b. It is found that the difference ratio increases, and reaches a plateau at about 5.5% for tensile deformation, while this parameter increases, and reaches a plateau at only about 2.7% for compressive deformation. It is apparent that the plateau in tension mode has a larger value than in compression mode. As we know, there is usually a larger yield stress in compression mode; therefore, we conclude that the less the FVs increase in size, the higher the yield stress is.

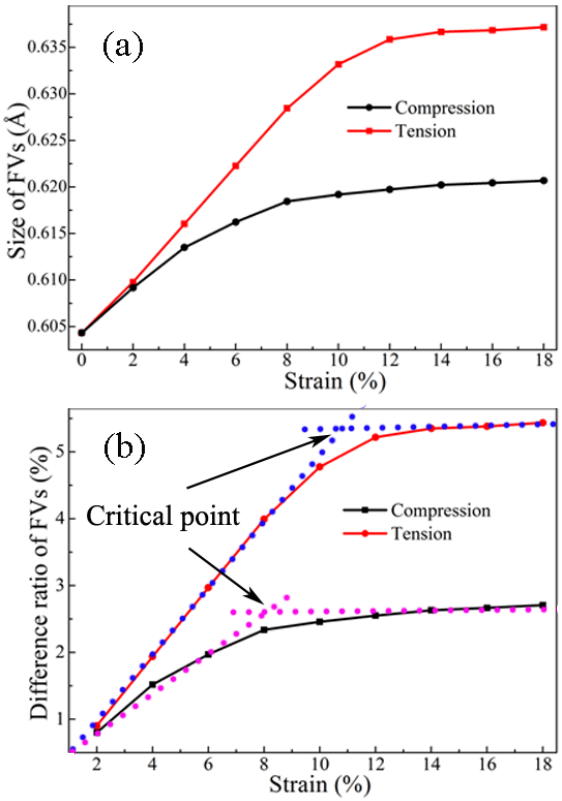


**Figure 4.** (Color online) Relations between FVs (free volumes; large voids whose radii are larger than 0.4 Å) and strain in tension and compression modes, including (**a**) the average sizes of FVs and (**b**) the difference ratio of FV sizes in different strains. The dotted lines are two straight lines indicating the approximate relations between FVs and strain.

A more interesting phenomenon is observed, whereby there is a critical point indicating the change of the linear relation between FV difference ratio and strain. In compression mode, this critical point has a strain value of 8%, which corresponds to the yield stress. Meanwhile, this critical point in the tension mode has a strain value of 11%, which is far removed from that (8%) corresponding to the yield stress. In other words, FVs do not obviously expand following yield stress during compressive deformation, while FVs continue to expand after the yield stress, probably until they reach the quasi-steady flow stress under tension. This may contribute significantly to the different mechanical behaviors between compressive and the tensile deformations; in particular, the difference in yield stress, and the difference in change until the quasi-steady flow stress is reached.

We checked the stress along *y*- and *z*-axis. The *y*- or *z*-direction stress keeps a relatively low value—less than 1 MPa—which is much smaller than that of the *x*-axis. This indicates that *y*- or *z*-direction stress does not significantly affect VC or FV parameters.

It has been suggested that the unique mechanical and physical properties of MGs are related to their structural stability [39–41]. Recent studies have shown that atomic packing is an important factor affecting the properties of MGs [42]. It is known that FVs are associated with atomic packing [21]. In this work, we have revealed that there is an expansion saturation of FVs in both compressive and tensile deformations, which may be due to the lower limit of loose atomic packing in the glassy state. The different evolutions of FVs between compressive and tensile deformations are probably due to the differences in atomic-level packing between these two deformations.

Furthermore, the changes of total FV in both tension and compression are illustrated in Figure 5. It is found that the total FV decreases with an increase of strain in compression, which is the opposite of the case in tension. Although we have revealed that the average size of FVs increases during compression, the number of FVs is largely reduced with an increase in strain. As a result, the total FV during compression decreases with an increase in strain. We suppose that, during compression, relatively small FVs are apt to merge into relatively large ones, leading to a decrease in FV number and an increase in FV size.

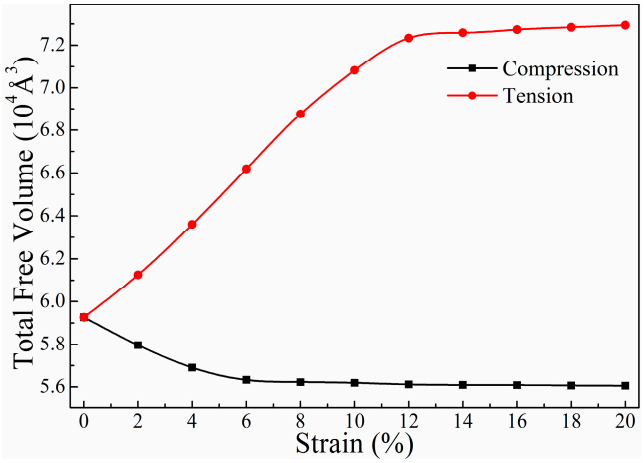


**Figure 5.** (Color online) Relations between total FVs and strain in tension and compression modes.

In this work, the yield behaviors in the simulated tension and compression are different, which is a topic studied previously in a Nature Materials article [16]. In this Nature Materials article, a fundamental yield criterion for an elementary STZ was proposed, which reveals that the physical origin of this effect in metallic glasses lies in the principle of 'atomistic friction', as embodied in the Mohr-Coulomb criterion. It is suggested that FV parameters, which are the focus of study in this work, should also have a close relation with STZ. Therefore, our FV result should be related to the Mohr-Coulomb criterion. There is interesting future work to be done on how FVs contribute to the deformation in MGs, according to the Mohr-Coulomb criterion.

In addition, it is known that sample size significantly affects the mechanical properties—in particular, the plasticity of MGs, as observed in many experimental investigations [43,44]. With regard to the simulation work, the model size is much smaller than those in the experimental samples; thus, the calculated stress-strain curve is usually different from its corresponding experimental one. However, as mentioned above, there are similar yield differences between tension and compression modes for both experimental and simulation investigation [5–7]. Therefore, this work studying the yield behaviors via the MD simulation is helpful for understanding the yield behaviors of real samples.

## 4. Conclusions

In this work, a new computational method for quantitatively detecting FVs is developed, based on which the fundamental structural mechanisms affecting the yield stage in tension and compression are investigated. It is revealed that the size of FVs increases with the strain in both tension and compression, while FVs have a lower expansion saturation value in compression than in tension, contributing to the higher yield strength in the former. In addition, the saturation value in compression/tension matches/mismatches the strain of 8%, corresponding to the yield strength, which could explain why there are different yield behaviors between these two deformation modes. This work sheds light on the unique mechanical properties of glassy alloys from an atomic-level structural perspective.

**Acknowledgments:** The authors would like to thank the HASYLAB (Hamburg Synchrotron Radiation Laboratory) in Germany, the Shanghai Synchrotron Radiation Facility in China, and the National Synchrotron Radiation Laboratory of China for the use of the advanced synchrotron radiation facilities. Financial support from the National Natural Science Foundation of China (Grant No. 51471088 and U1332112), the Fundamental Research Funds for the Central Universities (Grant No. NE2015004) and the project funded by the Priority Academic Program Development (PAPD) of Jiangsu Higher Education Institutions is gratefully acknowledged.

**Author Contributions:** Pengwei Wang performed simulation work upon the experimental data. Liang Yang performed analysis of this work and modified the article. Haiyang Li contributed to the experimental research work.

**Conflicts of Interest:** The authors declare no conflict of interest.

## References

1. Johnson, W.L. Bulk glass-forming metallic alloys: Science and technology. *MRS Bull.* **1999**, *24*, 42–56. [CrossRef]
2. Inoue, A. Stabilization of metallic supercooled liquid and bulk amorphous alloys. *Acta Mater.* **2000**, *48*, 279–306. [CrossRef]
3. Schuh, C.A.; Hufnagel, T.C.; Ramamurty, U. Mechanical behavior of amorphous alloys. *Acta Mater.* **2007**, *55*, 4067–4109. [CrossRef]
4. Sergueeva, A.V.; Mara, N.A.; Branagan, D.J.; Mukherjee, A.K. Strain rate effect on metallic glass ductility. *Scr. Mater.* **2004**, *50*, 1303–1307. [CrossRef]
5. Zhang, Z.F.; Eckert, J.; Schultz, L. Difference in compressive and tensile fracture mechanisms of $Zr_{59}Cu_{20}Al_{10}Ni_8Ti_3$ bulk metallic glass. *Acta Mater.* **2003**, *51*, 1167–1179. [CrossRef]
6. Qiu, K.Q.; Wang, A.M.; Zhang, H.F.; Ding, B.Z.; Hu, Z.Q. Mechanical properties of tungsten fiber reinforced ZrAlNiCuSi metallic glass matrix composite. *Intermetallics* **2002**, *10*, 1283–1288. [CrossRef]
7. Park, K.W.; Fleury, E.; Seok, H.K.; Kim, Y.C. Deformation behaviors under tension and compression: Atomic simulation of $Cu_{65}Zr_{35}$ metallic glass. *Intermetallics* **2011**, *19*, 1168–1173. [CrossRef]
8. Ogata, S.; Shimizu, F.; Li, J.; Wakeda, M.; Shibutani, Y. Atomistic simulation of shear localization in Cu-Zr bulk metallic glass. *Intermetallics* **2006**, *14*, 1033–1037. [CrossRef]
9. Feng, S.D.; Chan, K.C.; Chen, S.H.; Zhao, L.; Liu, R.P. The role of configurational disorder on plastic and dynamic deformation in $Cu_{64}Zr_{36}$ metallic glasses: A molecular dynamics analysis. *Sci. Rep.* **2017**, *7*, 40969. [CrossRef] [PubMed]
10. Spaepen, F. A microscopic mechanism for steady state inhomogeneous flow in metallic glasses. *Acta Metall.* **1977**, *25*, 407–415. [CrossRef]
11. Argon, A.S. Plastic deformation in metallic glasses. *Acta Metall.* **1979**, *27*, 47–58. [CrossRef]

12. Jiao, W.; Sun, B.A.; Wen, P.; Bai, H.Y.; Kong, Q.P. Crossover from stochastic activation to cooperative motions of shear transformation zones in metallic glasses. *Appl. Phys. Lett.* **2013**, *103*, 081904. [CrossRef]
13. Wang, W.H. Correlations between elastic moduli and properties in bulk metallic glasses. *J. Appl. Phys.* **2006**, *99*, 93506. [CrossRef]
14. Huang, B.; Bai, H.Y.; Wang, W.H. Unique properties of CuZrAl bulk metallic glasses induced by microalloying. *J. Appl. Phys.* **2011**, *110*, 123522. [CrossRef]
15. Cao, A.J.; Cheng, Y.Q.; Ma, E. Structural processes that initiate shear localization in metallic glass. *Acta Mater.* **2009**, *57*, 5146–5155. [CrossRef]
16. Schuh, C.A.; Lund, A.C. Atomistic basis for the plastic yield criterion of metallic glass. *Nat. Mater.* **2003**, *2*, 449–452. [CrossRef] [PubMed]
17. Levchenko, E.V.; Evteev, A.V.; Kozubski, R.; Belova, I.V.; Murch, G.E. Molecular dynamics simulation of surface segregation in a (110) B2-NiAl thin film. *Phys. Chem. Chem. Phys.* **2011**, *13*, 1214–1221. [CrossRef] [PubMed]
18. Sastry, S.; Corti, D.S.; Debenedeti, P.G.; Stillinger, F.H. Statistical geometry of particle packings. *Phys. Rev. E* **1997**, *56*, 5524–5532. [CrossRef]
19. Li, F.; Liu, X.J.; Hou, H.Y.; Chen, G.; Chen, G.L.; Li, M. Atomic scale calculation of the free volume in $Zr_2Ni$ metallic glass. *Intermetallics* **2009**, *17*, 98–103. [CrossRef]
20. Yang, L.; Guo, G.Q.; Chen, L.Y.; Huang, C.L.; Ge, T.; Chen, D.; Liaw, P.K.; Saksl, K.; Ren, Y.; Zeng, Q.S.; et al. Atomic-scale mechanisms of the glass-forming ability in metallic glasses. *Phys. Rev. Lett.* **2012**, *109*, 105502. [CrossRef] [PubMed]
21. Park, K.W.; Jang, J.; Wakeda, M.; Shibutani, Y.; Lee, J.C. Atomic packing density and its influence on the properties of Cu-Zr amorphous alloys. *Scr. Mater.* **2007**, *57*, 805–808. [CrossRef]
22. Wakeda, M.; Shibutani, Y.; Ogata, S. Relationship between local geometrical factors and mechanical properties for Cu-Zr amorphous alloys. *Intermetallics* **2007**, *15*, 139–144. [CrossRef]
23. Sun, Y.L.; Shen, J.; Valladares, A.A. Atomic structure and diffusion in $Cu_{60}Zr_{40}$ metallic liquid and glass: Molecular dynamics simulations. *J. Appl. Phys.* **2009**, *106*, 73520. [CrossRef]
24. Wu, S.Q.; Wang, C.Z.; Hao, S.G.; Zhu, Z.Z.; Ho, K.M. Energetics of local clusters in $Cu_{64.5}Zr_{35.5}$ metallic liquid and glass. *Appl. Phys. Lett.* **2010**, *97*, 21901. [CrossRef]
25. Bharathula, A.; Luo, W.; Windl, W.; Flores, K.M. Characterization of open volume regions in a simulated Cu-Zr metallic glass. *Metall. Mater. Trans. A* **2008**, *39*, 1779–1785. [CrossRef]
26. Duan, G.; Xu, D.H.; Zhang, Q.; Zhang, G.Y.; Cagin, T.; Johnson, W.L.; Goddard, W.A. Molecular dynamics study of the binary $Cu_{46}Zr_{54}$ metallic glass motivated by experiments: Glass formation and atomic-level structure. *Phys. Rev. B* **2005**, *72*, 224208. [CrossRef]
27. Sheng, H.W.; Luo, W.K.; Alamgir, F.M.; Bai, J.M.; Ma, E. Atomic packing and short-to-medium-range order in metallic glasses. *Nature* **2006**, *439*, 419–425. [CrossRef] [PubMed]
28. Mendelev, M.I.; Sordelet, D.J.; Kramer, M.J. Using atomistic computer simulations to analyze X-ray diffraction data from metallic glasses. *J. Appl. Phys.* **2007**, *102*, 43501. [CrossRef]
29. Hoover, W.G. Canonical dynamics: Equilibrium phase-space distributions. *Phys. Rev. A* **1985**, *31*, 1695–1697. [CrossRef]
30. Wang, X.D.; Ruta, B.; Xiong, L.H.; Zhang, D.W.; Chushkin, Y.; Sheng, H.W.; Lou, H.B.; Cao, Q.P.; Jiang, J.Z. Free-volume dependent atomic dynamics in beta relaxation pronounced La-based metallic glasses. *Acta Mater.* **2015**, *99*, 290–296. [CrossRef]
31. Park, K.W.; Shibutani, Y.; Falk, M.L.; Lee, B.J.; Lee, J.C. Shear localization and the plasticity of bulk amorphous alloys. *Scr. Mater.* **2010**, *63*, 231–234. [CrossRef]
32. Cheng, Y.Q.; Cao, A.J.; Sheng, H.W.; Ma, E. Local order influences initiation of plastic flow in metallic glass: Effects of alloy composition and sample cooling history. *Acta Mater.* **2008**, *56*, 5263–5275. [CrossRef]
33. Park, K.W.; Lee, C.M.; Wakeda, M.; Shibutani, Y.; Falk, M.L.; Lee, J.C. Elastostatically induced structural disordering in amorphous alloys. *Acta Mater.* **2008**, *56*, 5440–5450. [CrossRef]
34. Brostow, W.; Chybicki, M.; Laskowski, R. Voronoi polyhedra and Delaunay simplexes in the structural analysis of molecular-dynamics-simulated materials. *Phys. Rev. B* **1998**, *57*, 13448–13458. [CrossRef]
35. Tsai, A.P. Icosahedral clusters, icosaheral order and stability of quasicrystals—A view of metallurgy. *Sci. Technol. Adv. Mater.* **2008**, *9*. [CrossRef] [PubMed]

36. Sietsma, J.; Thijsse, B.J. Characterization of free volume in atomic models of metallic glasses. *Phys. Rev. B* **1995**, *52*, 3248–3255. [CrossRef]
37. Cui, X.; Zu, F.Q.; Zhang, W.J. Phase competition of $Cu_{64}Zr_{36}$ and its effect on glass forming ability of the alloy. *Cryst. Res. Technol.* **2013**, *48*, 11–15. [CrossRef]
38. Kramer, M.J.; Xu, M.; Ye, Y.Y.; Sordelet, D.J.; Morris, J.R. Phase stability and transformations in the $Zr_2Ni_xCu_{1-x}$ Amorphous System. *Metall. Mater. Trans. A* **2007**, *39*, 1847–1856. [CrossRef]
39. Cheung, T.L.; Shek, C.H. Thermal and mechanical properties of Cu-Zr-Al bulk metallic glasses. *J. Alloys Compd.* **2007**, *434*, 71–74. [CrossRef]
40. Ray, R.; Tanner, L.E. Metallic glasses with high strengths and high crystallization temperatures. *J. Mater. Sci.* **1980**, *15*, 1599–1600. [CrossRef]
41. Zhang, W.; Qin, C.; Zhang, X.; Inoue, A. Effects of additional noble elements on the thermal stability and mechanical properties of Cu-Zr-Al bulk glassy alloys. *Mater. Sci. Eng. A* **2007**, *449*, 631–635. [CrossRef]
42. Fan, C.; Liaw, P.K.; Wilson, T.W.; Dmowski, W.; Choo, H.; Liu, C.T.; Richardson, J.W.; Proffen, T. Structural model for bulk amorphous alloys. *Appl. Phys. Lett.* **2006**, *89*, 111905. [CrossRef]
43. Huang, Y.J.; Shen, J.; Sun, J.F. Bulk metallic glasses: Smaller is softer. *Appl. Phys. Lett.* **2007**, *90*, 81919. [CrossRef]
44. Wu, F.F.; Zhang, Z.F.; Mao, S.X. Size-dependent shear fracture and global tensile plasticity of metallic glasses. *Acta Mater.* **2009**, *57*, 257–266. [CrossRef]